Complex-temperature singularities in Potts models on the square lattice

Victor Matveev* and Robert Shrock†
Institute for Theoretical Physics, State University of New York at Stony Brook, Stony Brook, New York 11794-3840
(Received 28 May 1996)

We report some results on the complex-temperature (CT) singularities of q-state Potts models on the square lattice. We concentrate on the problematic region $\mathrm{Re}(a)<0$ (where $a=e^K$) in which CT zeros of the partition function are sensitive to finite lattice artifacts. From analyses of low-temperature series expansions for $3\leq q\leq 8$, we establish the existence, in this region, of complex-conjugate CT singularities at which the magnetization and susceptibility diverge. From calculations of zeros of the partition function, we obtain evidence consistent with the inference that these singularities occur at endpoints a_e, a_e^* of arcs protruding into the (complex-temperature extension of the) ferromagnetic phase. Exponents for these singularities are determined; e.g., for $q=3$, we find $\beta_e=-0.125(1)$, consistent with $\beta_e=-1/8$. By duality, these results also imply associated arcs extending into the (CT extension of the) symmetric paramagnetic phase. Analytic expressions are suggested for the positions of some of these singularities; e.g., for $q=5$, our finding is consistent with the exact value $a_e, a_e^*=2(-1\mp i)$. Further discussions of complex-temperature phase diagrams are given. [S1063-651X(96)09412-3]

PACS number(s): 05.20.−y, 05.50.+q, 64.60.Cn, 75.10.Hk

I. INTRODUCTION AND MODEL

In this paper, we report some results on complex-temperature singularities of the q-state Potts model [1,2] on the square lattice. The Potts model has been of interest both as an example of a particular universality class for critical phenomena and as a model for physical phenomena such as the adsorption of certain gases on substrates [3]. However, in contrast to the two-dimensional (2D) Ising model (equivalent to the $q=2$ case), the free energy of the Potts model for general q has never been calculated in closed form, even for zero external field(s). Some exact results have been established for the model: from a duality relation, the critical point separating the disordered, Z_q-symmetric high-temperature phase from the low-temperature phase with spontaneously broken Z_q symmetry and associated nonzero ferromagnetic (FM) long-range order is known [1]. The free energy, latent heat [4], and magnetization [5] have been calculated exactly by Baxter at this critical point, establishing that the model has a continuous, second-order transition for $q\leqslant 4$ and a first-order transition for $q\geqslant 5$. Baxter has also shown that although the $q=3$ model has no phase with antiferromagnetic (AFM) long-range order at any finite temperature, there is an AFM critical point at $T=0$ [5]. The values of the critical exponents (for the range of q where the transition is continuous) have been determined [6]. Subsequently, further insight into the critical behavior was gained using the methods of conformal field theory [7]. A review of work up through 1982 was given in Ref. [8].

In general, if one knew the exact (zero-field) free energy, one would be able to determine the full phase diagram as a function of complex temperature. The idea of generalizing a variable on which the free energy depends from real physical values to complex values was pioneered by Yang and Lee [9]. These authors considered the generalization of the external magnetic field to complex values [9] and proved a celebrated theorem that the complex-field zeros of the Ising model partition function lie on the unit circle in the μ plane, where $\mu=e^{-2\beta H}$, pinching the real axis as the temperature T decreases through the critical point T_c. Complex-temperature (CT) singularities of Ising models, first considered in Ref. [10], were investigated both by means of CT zeros of the partition function [11–13] and via their effects on low-temperature series expansions [14]. As well as being of historical interest, these are relevant here because of the equivalence of the (spin-1/2) Ising model and $q=2$ Potts model. There is continuing interest in such complexifications because of the deeper insight that they give one into the properties of statistical-mechanical models (for the Ising model, see, e.g., Refs. [15–26]). From general arguments and comparisons with exact solutions for 2D Ising models with isotropic couplings, one knows that in the thermodynamic limit, CT zeros merge together to form curves (including possible line segments) across which the free energy is nonanalytic. These curves form the complex-temperature phase boundary $\mathcal{B}$ of the model. One can define notions of complex-temperature extensions of the physical paramagnetic (PM), FM, and (if it occurs) AFM phases. In certain cases there are other (labeled O) complex-temperature phases that do not have any overlap with any physical phase. These various CT phases are separated by boundaries comprising $\mathcal{B}$. The locus of points making up $\mathcal{B}$ may also contain part(s) consisting of curves (arcs) or line segments that protrude into and terminate in certain phases.

There have been several calculations of complex-temperature zeros of the partition function for the Potts model on the square lattice [27–32]. Since the early calculations for $q=3,4$, it has been recognized that the zeros show one clear feature: if one uses duality-preserving boundary conditions, then in the $\mathrm{Re}(a)>0$ region (where $a=e^K$; see below for notation), these zeros lie on a portion of the unit circle $|x|=1$, where $x=(a-1)/\sqrt{q}$ [28–31]. In passing, we

*Electronic address: vmatveev@insti.physics.sunysb.edu
†Electronic address: shrock@insti.physics.sunysb.edu

note that in the $q\to\infty$ limit it has been shown (assuming that the $q\to\infty$ limit and the thermodynamic limit commute) that the CT zeros lie on the unit circle $|x|=1$ [32,33]. However, for a given (finite) q, the situation in the $\mathrm{Re}(a)<0$ region has proved to be much more difficult to elucidate. The zeros exhibit considerable scatter and, as we shall demonstrate, significant sensitivity to the boundary conditions used for the finite lattice calculations, even if one requires these to preserve duality. These facts have rendered it problematic to try to make inferences from calculations of zeros on finite lattices about the complex-temperature phase boundary $\mathcal{B}$ in the thermodynamic limit. In one early work [27] it was conjectured that in the thermodynamic limit the zeros lie on the two circles $|a-1|=\sqrt{q}$ and $|a+1|=\sqrt{4-q}$ for $q=3$ and $q=4$ (where the second circle degenerates to a point), but shortly thereafter, from a calculation of zeros for the $q=3$ model on larger lattices, it was concluded that this conjecture was false [28] and the zero distribution did not suggest the existence of any simple algebraic expression that would describe this distribution. The same conclusion was reached from a calculation of the zeros for the $q=4$ model [29].

We have been able to make progress in the problematic $\mathrm{Re}(a)<0$ region by employing a powerful method not hitherto used for this purpose, viz., to combine analyses of low-temperature series with calculations of CT zeros of the partition function. We report our results here. In our series work, we have taken advantage of the recent calculations of quite long low-temperature series for the free energy, magnetization, and susceptibility of the square-lattice Potts model for $q=3$ up to $q=10$ by Briggs, Enting, and Guttmann [35], extending earlier calculations (e.g., Ref. [36]; for $q=3$ and $q=8$, see also Ref. [37]). The organization of this paper is as follows. In Sec. II we define the model and our notation and mention some of the general exact results that are known. In Secs. III and IV we present our results for the $q=3$ and $q=4$ Potts model. In Sec. V we mention some similar results for $q\geq 5$ Potts models. Concluding remarks are given in Sec. VI.

II. DEFINITION OF MODEL AND EXACT RESULTS

The (isotropic, nearest-neighbor) q-state Potts model on a lattice Λ is defined, at a temperature T, by the partition function

$$Z=\sum_{\{\sigma_n\}} e^{-\beta\mathcal{H}}, \tag{1}$$

with the Hamiltonian

$$\mathcal{H}=-J\sum_{\langle nn'\rangle}\delta_{\sigma_n\sigma_{n'}}-H\sum_n \delta_{0\sigma_n}, \tag{2}$$

where $\sigma_n=0,\ldots,q-1$ are Z_q-valued variables on each site $n\in\Lambda$; $\beta=(k_BT)^{-1}$; and $\langle nn'\rangle$ denotes pairs of nearest-neighbor sites. We use the notation $K=\beta J$, $h=\beta H$,

$$a=z^{-1}=e^K, \tag{3}$$

and

$$x=\frac{e^K-1}{\sqrt{q}} \tag{4}$$

and denote the (reduced) free energy per site as $f=-\beta F=\lim_{N_s\to\infty}N_s^{-1}\ln Z$, where N_s denotes the number of sites in the lattice. Here we consider the square lattice. There are actually q types of external fields that one may define, favoring the respective values $\sigma_n=0,\ldots,q-1$; it suffices for our purposes to include only one. The order parameter is defined to be

$$m=\frac{qM-1}{q-1}, \tag{5}$$

where $M=\langle\sigma\rangle=\lim_{h\to 0}\partial f/\partial h$. With this definition, $m=0$ in the Z_q-symmetric, disordered phase and $m=1$ in the limit of saturated FM long-range order. We shall refer to m as the magnetization. Finally, the (reduced, initial) susceptibility is denoted as $\overline{\chi}=\beta^{-1}\chi=\partial m/\partial h|_{h=0}$. We consider the zero-field model $H=0$ unless otherwise stated.

The general q-state Potts model on the square lattice obeys the duality relation [1]

$$(a-1)(a_d-1)=q, \tag{6}$$

where $a_d\equiv\mathcal{D}(a)$ is the image under the duality map $\mathcal{D}$ of a,

$$\mathcal{D}(a)=1+\frac{q}{a-1}, \tag{7}$$

with $\mathcal{D}^2=1$ as usual. In terms of the variable x, this duality relation takes the simple form

$$x_d=\frac{1}{x}. \tag{8}$$

The critical point at which a phase transition occurs between the high-temperature symmetric phase and the low-temperature FM phase is given by the self-dual point $x_c=1$, i.e., $a_c=1+\sqrt{q}$. One may observe that Eq. (6) also has a second self-dual solution at a complex-temperature point

$$a=1-\sqrt{q}\equiv a_l. \tag{9}$$

Exact expressions for the free and internal energy, latent heat, and magnetization have been given by Baxter [4,5] on the critical self-dual curve

$$(a-1)^2=q. \tag{10}$$

Since the latent heat is zero at a_c for $q\leq 4$ [4], the corresponding transition between the symmetric and FM phases is continuous. The curve (10) also includes the complex-temperature singular point at a_l in Eq. (9). We note that by the same reasoning, the phase boundary associated with the complex-temperature point a_l is also continuous. Exact results have also been given by Baxter for the critical manifold [5,38]

$$(a+1)^2=4-q. \tag{11}$$

For $q=3$, Eq. (11) has two solutions: the AFM critical point at $a=0$, i.e., $T=0$ with $J<0$, and a complex-temperature point

$$a=-2\equiv a_s. \tag{12}$$

We observe that these two points are mapped onto each other under the duality mapping $\mathcal{D}$:

$$\mathcal{D}(a=0)=-2. \tag{13}$$

For $q=4$, Eq. (11) has only the solution $a=-1$, implying that for $q\geq 4$ the model has no AFM long-range order even at $T=0$.

Consider an $L_x\times L_y$ planar square lattice G with $N_s\equiv N_0$ sites (0-cells), $N_b\equiv N_1$ bonds (1-cells), and $N_p\equiv N_2$ plaquettes (2-cells). We shall discuss boundary conditions in Sec. III E below. The dual of G, which we denote $G_d=\mathcal{D}(G)$, is defined by associating uniquely a $(2-p)$-cell of G_d with each p-cell of G, so that $(N_0)_G=(N_2)_{G_d}$, $(N_1)_G=(N_1)_{G_d}$, and $(N_2)_G=(N_0)_{G_d}$. Since the planar graph has no handles, $N_h=0$, and hence Euler characteristic $\chi_E=2(1-N_h)=2$, it follows from the Euler relation $\Sigma_{j=0}^{2}(-1)^j N_j=\chi_E$ that $N_0-N_1+N_2=2$. The duality relation connecting the partition function Z_G on G with that on G_d is [8]

$$Z_G(x)=x^{N_1}q^{N_0-1-(1/2)N_1}Z_{G_d}(x_d). \tag{14}$$

It follows from (14) that in the thermodynamic limit, the singularities of that the free energy at a point a and its dual image a_d are the same. In particular,

$$f_{\rm sing}(q=3;a=-2)=f_{\rm sing}(q=3;a=0). \tag{15}$$

In discussing the complex-temperature phase diagram, it is convenient to use the Boltzmann weight z, its inverse a, and the related variable x. For $q=3$, the exact results discussed above show that the phase structure for physical temperature (i.e., $0\leq a\leq\infty$) consists of (i) the disordered, Z_3-symmetric PM phase for $0<a\leq 1+\sqrt{3}$, (ii) the FM phase for $1+\sqrt{3}<a\leq\infty$, and (iii) an AFM critical point at $a=0$. For $q\geq 4$, the physical phase structure consists only of the PM phase for $0\leq a\leq 1+\sqrt{q}$ and the FM phase for $1+\sqrt{q}<a\leq\infty$. One defines the complex-temperature extensions (CTE's) of the PM and FM phases by analytically continuing away from the respective segments of the positive real a axis. Two rigorous properties are the following. First, because the model has a high-temperature series expansion with finite radius of convergence, it follows that the CTE of the PM phase occupies a finite neighborhood surrounding the point $a=1$. Second, it is easy to show that for sufficiently large $|a|$, one is necessarily in the (CTE of the) FM phase. To see this, let $a=\rho_a e^{i\theta_a}$; then

$$K=\ln a=\ln\rho_a+i(\theta_a+2\pi n), \tag{16}$$

where n denotes the Riemann sheet of the logarithm and may be taken to be equal to zero here. It is clear that for sufficiently large $|a|=\rho_a$, the angle θ_a makes a negligible contribution to K, so that (given that $d=2$ is above the lower critical dimensionality for the FM transition) the system will be in the FM phase. This fact can be seen equivalently as a consequence of the fact that the model has a low-temperature expansion with a finite radius of convergence, so that there is a finite neighborhood of the origin in the complex z plane where it is in the (CTE of the) FM phase. Henceforth, we shall generally refer to the complex-temperature extension of the FM phase simply as the FM phase and similarly with the PM phase.

III. $q=3$ POTTS MODEL

We shall discuss our methods in detail for the $q=3$ square-lattice Potts model and then proceed to the higher-q cases. We begin with analyses of the low-temperature series expansions. The series for the partition function, magnetization, and susceptibility have been calculated to order z^{47} [35]. As in our previous studies of complex-temperature singularities of various spin models, we have used both d log Padé and differential approximants to analyze the series. We fit the specific heat C, the magnetization m, and the (reduced) susceptibility χ to the leading singular forms applicable near a generic singular point $z_{\rm sing}$:

$$C\sim(1-z/z_{\rm sing})^{-\alpha'_{\rm sing}}, \tag{17}$$

$$m\sim(1-z/z_{\rm sing})^{\beta_{\rm sing}}, \tag{18}$$

and

$$\overline{\chi}\sim(1-z/z_{\rm sing})^{-\gamma'_{\rm sing}}. \tag{19}$$

As usual, the primes indicate that we are approaching this singularity from within the interior of the FM phase. We find convincing evidence from our series analyses for singularities at two complex-conjugate points, which we denote z_e and z_e^*, at which the magnetization, susceptibility, and specific heat are divergent.

A. Magnetization

In Table I we present some diagonal and near-diagonal d log Padé results for this singularity. (We have, of course, also calculated approximants farther from the diagonal.) It should be noted that the actual values of β_e have small imaginary parts; we list only the real part since, from our previous experience with complex-temperature singularities in the Ising model [19–22], when these are probed to very high accuracy, the exponents extrapolate to real values. Our analysis of the series for the order parameter indicates complex-conjugate singularities at approximately $z_e, z_e^*=-0.34\pm 0.29i$ (the location will be discussed further below), where m diverges with the exponent

$$\beta_e=-0.125(1). \tag{20}$$

A plausible inference is that the exact value of this exponent is

$$\beta_e=-\frac{1}{8}. \tag{21}$$

TABLE I. Values of z_e and β_e from d log Padé approximants to low-temperature series for m for $q=3$.

$[N/D]$	z_e	β_e
[13/12]	$-0.340504+0.287457i$	-0.1258
[13/13]	$-0.340420+0.287491i$	-0.1256
[14/13]	$-0.340382+0.287392i$	-0.1250
[13/14]	$-0.340358+0.287473i$	-0.1252
[14/14]	$-0.340441+0.287408i$	-0.1254
[15/14]	$-0.340428+0.287382i$	-0.1252
[14/15]	$-0.340427+0.287365i$	-0.1251
[15/15]	$-0.340433+0.287339i$	-0.1251
[16/15]	$-0.340436+0.287386i$	-0.1253
[15/16]	$-0.340429+0.287368i$	-0.1252
[16/16]	$-0.340512+0.287332i$	-0.1256
[17/16]	$-0.340405+0.287364i$	-0.1250
[16/17]	$-0.340412+0.287339i$	-0.1250
[17/17]	$-0.340406+0.287354i$	-0.1250
[18/17]	$-0.340416+0.287357i$	-0.1251
[17/18]	$-0.340410+0.287350i$	-0.1250
[18/18]	$-0.340406+0.287356i$	-0.1250
[19/18]	$-0.340407+0.287363i$	-0.1250
[18/19]	$-0.340376+0.287413i$	-0.1251
[19/19]	$-0.340312+0.287325i$	-0.1244
[20/19]	$-0.340260+0.287344i$	-0.1241
[19/20]	$-0.340273+0.287344i$	-0.1242
[20/20]	$-0.340305+0.287229i$	-0.1241
[21/20]	$-0.340285+0.287321i$	-0.1242
[20/21]	$-0.340292+0.287319i$	-0.1243
[21/21]	$-0.340326+0.287269i$	-0.1243
[22/21]	$-0.340711+0.286857i$	-0.1246
[22/22]	$-0.340855+0.286878i$	-0.1247
[23/22]	$-0.340688+0.286888i$	-0.1246
[22/23]	$-0.340982+0.287191i$	-0.1260
[23/23]	$-0.340806+0.287311i$	-0.1262

TABLE II. Values of z_e and γ_e' from d log Padé approximants to low-temperature series for $\overline{\chi}$ for $q=3$.

$[N/D]$	z_e	γ_e'
[15/15]	$-0.337324+0.290677i$	1.123
[17/15]	$-0.339008+0.289393i$	1.190
[15/16]	$-0.339062+0.288573i$	1.173
[16/16]	$-0.338269+0.289319i$	1.149
[17/16]	$-0.338281+0.289318i$	1.150
[18/16]	$-0.338121+0.289177i$	1.138
[15/17]	$-0.337814+0.289264i$	1.125
[16/17]	$-0.338280+0.289318i$	1.150
[17/17]	$-0.338270+0.289319i$	1.149
[18/17]	$-0.338227+0.289314i$	1.147
[19/17]	$-0.338392+0.289613i$	1.163
[16/18]	$-0.338168+0.289263i$	1.143
[17/18]	$-0.338226+0.289312i$	1.147
[18/18]	$-0.338259+0.289325i$	1.149
[19/18]	$-0.338336+0.289377i$	1.154
[20/18]	$-0.338338+0.289242i$	1.151
[17/19]	$-0.338077+0.289273i$	1.138
[18/19]	$-0.338332+0.289360i$	1.153
[19/19]	$-0.338311+0.289333i$	1.152
[20/19]	$-0.338355+0.289392i$	1.155
[21/19]	$-0.338537+0.289589i$	1.170
[18/20]	$-0.338310+0.289320i$	1.151
[19/20]	$-0.338341+0.289364i$	1.154
[20/20]	$-0.338168+0.289333i$	1.145
[21/20]	$-0.337704+0.289629i$	1.126
[22/20]	$-0.337349+0.290843i$	1.111
[19/21]	$-0.338488+0.291209i$	1.196
[20/21]	$-0.337205+0.289884i$	1.102
[21/21]	$-0.340368+0.286150i$	1.080
[20/22]	$-0.336698+0.291093i$	1.064

We comment that although such a divergence in the order parameter is forbidden in usual physical phase transitions, it can and does occur at complex-temperature singularities. Indeed, in our previous work we have noted several instances where the magnetization diverges at CT singularities. For example, exact results show that M diverges [like $(1+3u)^{-1/8}$] at the CT point $u=-1/3$ in the (zero-field) spin-1/2 Ising model on the triangular lattice and at $u=u_e=-(3-2\sqrt{2})$ in the Ising model with $\beta H=i\pi/2$ on the square lattice [like $(1-u/u_e)^{-1/8}$] [22].

The appearance of the exponent (20) at this CT singularity in the square-lattice Potts model is intriguing since $-1/8$ is not a simple (negative) multiple of any of the physical magnetic exponents in the model. This contrasts with the above-mentioned examples from the 2D Ising model, where, as is clear from the exact solution, the divergent magnetic exponents at $u=-1/3$ on the triangular lattice and at $u=u_e$ on the square lattice for $h=i\pi/2$ are precisely minus the common value of $\beta=1/8$ at the physical PM-FM critical point. Specifically, for the PM-FM transition in the 2D $q=3$ Potts model, the thermal and magnetic exponents are $y_t=1/\nu=1/\nu'=6/5$ and $y_h=28/15$, whence $\alpha=\alpha'=2-d/y_t=1/3$, $\delta=(d/y_h-1)^{-1}=14$, $\beta=1/9$, $\gamma=\gamma'=13/9$, and $\eta=4/15$ [6,39]. One recalls that the exponent 1/8 does occur in the set of the conformal weights for the $m=5$ conformal field theory relevant to the 2D $q=3$ Potts model, viz., $h_{1,2}=h_{4,4}=1/8$, where $h_{p,q}=\{[(m+1)p-mq]^2-1\}/[4m(m+1)]$ for $p=1,\ldots,m-1$ and $q=1,\ldots,p$ and the central charge is given by $c=1-6/[m(m+1)]$ and has the value $c=4/5$ for this case [7]. However, the relation of this to the appearance of the exponent $-1/8$ at the complex-temperature singularities z_e, z_e^* is obscure, for several reasons. First, as we discussed in Ref. [19], there are violations of basic scaling relations at complex-temperature singularities, so that it is not clear how to apply conformal field theory to such singularities (since CFT implies, among other things, such scaling relations). Second, since the Hamiltonian is not real at complex-temperature singularities, it is not obvious why the unitary rational conformal series is relevant to such singularities.

B. Susceptibility

In Table II we present our corresponding results from the d log Padé analysis of the low-temperature series for the susceptibility. We have also carried out a similar study with (first-order, unbiased) differential approximants, which

TABLE III. Values of z_e and α_e' from differential approximants to low-temperature series for (reduced) specific heat $C/(k_B K^2)$ for $q=3$.

$[L/M_0;M_1]$	z_e	α_e'
[8/16;14]	$-0.3407788+0.2885827i$	1.072
[8/16;15]	$-0.3407563+0.2878427i$	1.052
[8/16;16]	$-0.3395542+0.2877949i$	0.997
[8/16;17]	$-0.3399969+0.2874121i$	0.986
[8/17;15]	$-0.3393125+0.2891874i$	0.960
[8/17;16]	$-0.3391475+0.2886514i$	0.967
[10/15;13]	$-0.3405761+0.2887910i$	1.049
[10/15;14]	$-0.3405514+0.2889317i$	1.044
[10/15;15]	$-0.3400580+0.2896685i$	0.987
[10/15;16]	$-0.3392558+0.2894922i$	0.935
[10/16;14]	$-0.3396813+0.2885613i$	0.989
[10/16;15]	$-0.3397607+0.2885435i$	0.994
[12/14;12]	$-0.3401737+0.2893914i$	1.001
[12/14;13]	$-0.3405823+0.2891851i$	1.049
[12/14;14]	$-0.3406363+0.2897800i$	1.059
[12/14;15]	$-0.3395286+0.2896329i$	0.934
[12/15;13]	$-0.3407441+0.2896263i$	1.071
[12/15;14]	$-0.3404562+0.2891536i$	1.039
[14/13;11]	$-0.3399260+0.2888016i$	0.989
[14/13;12]	$-0.3399969+0.2885408i$	1.001
[14/13;13]	$-0.3395575+0.2895497i$	0.919
[14/13;14]	$-0.3395242+0.2893949i$	0.915
[14/14;12]	$-0.3405031+0.2889864i$	1.030
[14/14;13]	$-0.3395982+0.2892116i$	0.942
[16/12;10]	$-0.3394602+0.2889824i$	0.955
[16/12;11]	$-0.3391883+0.2891054i$	0.929
[16/12;12]	$-0.3394838+0.2892739i$	0.939
[16/12;13]	$-0.3393726+0.2892381i$	0.934
[16/13;11]	$-0.3394488+0.2892846i$	0.937
[16/13;12]	$-0.3394364+0.2893045i$	0.933
[18/11;9]	$-0.3404461+0.2882994i$	1.032
[18/11;10]	$-0.3398013+0.2888885i$	0.979
[18/11;11]	$-0.3395252+0.2888272i$	0.962
[18/11;12]	$-0.3396986+0.2891254i$	0.955
[18/12;10]	$-0.3394656+0.2892506i$	0.939
[18/12;11]	$-0.3394441+0.2891136i$	0.945

yields the same value, to within the uncertainty. We determine the value of the specific heat exponent at the singularities z_e, z_e^* to be

$$\gamma_e' = 1.14(6), \tag{22}$$

where the uncertainty represents a theoretical estimate from the scatter of values among different Padé and differential approximants.

C. Specific heat

To study the complex-temperature singularities in the specific heat, we have again carried out analyses with both Padé and differential approximants. As an illustration, we show in Table III our results from the latter. Our notation is the same as in our earlier works, e.g. Ref. [19]; $[L/M_0;M_1]$ is the differential approximant to the generic function $\phi(z)$ obtained as the solution to the ordinary differential equation $Q_0(z)\phi(z)+Q_1(z)(zd/dz)\phi(z)=R(z)$, where Q_0, Q_1, and R are polynomials of order M_0, M_1, and L. A review of the methods is given in Ref. [40]. We determine the specific-heat exponent to be

$$\alpha_e' = 1.0(1). \tag{23}$$

As can be seen from Tables I–III, the magnetization, susceptibility, and specific-heat series give consistent values for the location of the singularities z_e, z_e^*. Combining these, we infer that

$$z_e, z_e^* = -0.339(2) \pm 0.289(2)i. \tag{24}$$

For our comparison with the plots of zeros of the partition function, it will be convenient to reexpress this in terms of the a and x variables. We list the results in Table IV (together with positions of the corresponding singularity for higher values of q, to be discussed later).

In passing, we observe that although we have found violations of scaling relations such as $\alpha+2\beta+\gamma=2$ and $\alpha'+2\beta+\gamma'=2$ in our previous work at various complex-temperature singularities (e.g., Refs. [19,24]), in the present case, we obtain $\alpha_e'+2\beta_e+\gamma_e'=1.9\pm0.1$ so that, to within the uncertainties, this exponent relation is satisfied.

D. Singularities at dual images of a_e, a_e^*

A rigorous consequence of the duality of the model is that the free energy also is singular, with the same singularity, at the points that are the dual images of the a_e and a_e^*, namely, for the central values $\mathcal{D}(a_e), \mathcal{D}(a_e^*) = 0.141 \pm 0.462i$ or, equivalently, $\mathcal{D}(x_e), \mathcal{D}(x_e^*) = -0.496 \pm 0.267$. These points lie in the (CTE) PM phase. Note that since $|x_c|=1$ while $|x_e|=0.56$, the singularities at x_e, x_e^* lie closer to the origin in the x plane than the physical critical point.

E. Connection of a_e, a_e^* singularities with CT phase boundary $\mathcal{B}$

We would also like to relate these complex-conjugate CT singularities at z_e, z_e^* or, equivalently, in the complex a plane, at a_e, a_e^*, to the complex-temperature phase boundary $\mathcal{B}$. From our previous studies on CT singularities [20,22,24], we formulated a conjecture that whenever an arc or line segment of the phase boundary protrudes into, and ends in, the FM phase, there is a divergence in M at the endpoint of this arc. We proved that this divergence in M implies also a divergence in χ at the same endpoint [24]. Besides the exact results alluded to above that exhibit this behavior, our calculations of partition function zeros for the 2D higher-spin square-lattice Ising model [23], in conjunction with the series analyses of Jensen, Guttmann, and Enting [26], are consistent with the conjecture. A natural extension of the conjecture is that the divergences which we have found in m at these CT points in the square-lattice q-state Potts model indicate that these points are endpoints of arcs of points where f is nonanalytic, i.e., arcs on the CT phase boundary $\mathcal{B}$.

TABLE IV. Values of z_e and, correspondingly, a_e and x_e from analyses of low-temperature series for magnetization, susceptibility, and specific heat. See the text for further details.

q	z_e, z_e^*	a_e, a_e^*	x_e, x_e^*
3	$-0.339(2) \pm 0.289(2)i$	$-1.71(1) \mp 1.46(1)i$	$-1.56(1) \mp 0.841(3)i$
4	$-0.288(2) \pm 0.270(2)i$	$-1.85(1) \mp 1.73(1)$	$-1.42(1) \mp 0.866(4)i$
5	$-0.251(2) \pm 0.251(2)i$	$-1.99(1) \mp 1.99(1)i$	$-1.34(1) \mp 0.891(4)i$

In order to test this conjecture here, we have carried out calculations of complex-temperature zeros of the partition function for several different finite lattices, using transfer matrix methods, as in our earlier study of partition function zeros for the 2D higher-spin Ising model [23]. At appropriate points we shall make comparison with previous computations of zeros for the square-lattice Potts model [28–31]. It is desirable to, and we shall, restrict ourselves to lattices with duality-preserving boundary conditions (DBC's) [8,30,31]. These guarantee that $\mathcal{D}(G)=G$, i.e., the dual of a (finite) lattice G is (isomorphic to) the original lattice. To discuss these, we recall Eq. (14) and the associated definitions. Note that 2D periodic, i.e., toroidal, boundary conditions do not preserve duality for a finite lattice. The boundary conditions are not uniquely specified by the condition that they preserve duality. One type, which we label as type 1, was discussed in Ref. [31] (see their Fig. 1). We shall need a straightforward generalization of it to the case of an $L_x \times L_y$ lattice with $L_x \neq L_y$, and we describe this as follows. Let the lattice be oriented with the x and y directions being horizontal and vertical, respectively. Let all of the sites on the upper and right-hand edges, including the corners, connect along directions outward from the lattice to a common site adjoined to this lattice (so that the upper right corner connects to this adjoined point via bonds in both the x and the y directions), while all of the sites on the lower and left-hand edges, excluding the previously mentioned corners, have free boundary conditions. For the dual lattice, the special adjoined point may be taken to lie to the lower left of the lattice. In Ref. [31] it was noted that from (unpublished) calculations of zeros with other DBC's, they obtained agreement with their conclusions from type-1 DBC's that for $\mathrm{Re}(x)>0$ the zeros lie on the circle $|x|=1$ [31]. We have also used a set of DBC's different from type 1, which we denote as type 2 [34]. For these, let the $L_x \times L_y$ lattice have periodic boundary conditions (PBC's) in the x direction, so that the lattice may be pictured as a cylinder with its axis oriented vertically. Now connect all of the sites on the upper edge of the cylinder to a special point adjoined to the lattice and let all of the sites on the lower edge of the cylinder have free boundary conditions. The dual lattice is constructed in the usual way, assigning sites to each 2-cell of the original graph and adjoining the special point below the cylinder with the stipulation that the points on the upper edge of the dual lattice have free boundary conditions and the points on the lower edge connect to the adjoined point. For both type-1 and type-2 DBC's, $N_0 = L_x L_y + 1 = N_2$ and $N_1 = 2L_x L_y$ so that the prefactor $q^{N_0 - 1 - (1/2)N_1} = 1$ in Eq. (14). Note also that both type-1 and type-2 DBC's force some sites to have coordination number 3 rather than 4 and the adjoined point has coordination number $L_x + L_y$ for type-1 DBC's and L_x for type-2 DBC's. This is in contrast to periodic boundary conditions, which violate duality but maintain equal coordination number for all lattice sites.

A third type of DBC has recently been suggested to us by Wu [34]; it can be defined as follows, and will be denoted as DBC type 3. Consider an $L_x \times L_y$ lattice with $L_x = L+1$, $L_y = L$. Let all of the sites on the longer (horizontal) upper edge of the lattice be connected to a special adjoined point, via $L+1$ bonds, and similarly let all of the sites on the lower edge of the lattice be connected by $L+1$ bonds to a second adjoined point. Finally, connect the two adjoined points by a single bond and let the sites on the vertical edges of the lattice have free boundary conditions (in the outward horizontal directions). This lattice has $N_0 = N_2 = L(L+1)+2$ and $N_1 = 2(L^2+L+1) = 2(N_0-1)$ [so again, $q^{N_0 - 1 - (1/2)N_1} = 1$ in (14)]. Evidently, type-3 DBC's share greater similarity with type 1 than type 2 since in types 1 and 3 no subsets of edge sites have periodic boundary conditions, while in type 2 the sites on the vertical edges do have PBC's. For a given value of q, the patterns of zeros that we have obtained with type-3 DBC's are indeed similar to those with type 1.

In Figs. 1(a) and 1(b) we present calculations of complex-temperature zeros, in the complex a plane, of the partition function for the $q=3$ Potts model on 8×10 lattices with duality-preserving boundary conditions of types 1 and 2, respectively. The positions of the singular points a_e, a_e^* are marked with small circles on both of these plots. A comparison of these plots gives a quantitative measure of how the positions of the zeros can vary for different boundary conditions and specifically for those that maintain duality. This extends previously published plots [30,31], which showed that the pattern of zeros differs significantly when one uses duality-preserving, as opposed to duality-violating, boundary conditions. These comparisons demonstrated that once one specializes to duality-preserving boundary conditions (BC's), the zeros in the $\mathrm{Re}(a)>0$ region lie nicely on the circle $|a-1| = \sqrt{q}$, whereas they lie close to, but not exactly on, this circle for duality-violating BC's. Among previously published calculations with duality-preserving BC's, there is one, given as Fig. 11.1 in Ref. [30], on a lattice as large as the one that we use and the pattern of zeros found there is very close to the pattern in our Fig. 1(b). In our figure, one can discern two outer-lying complex-conjugate arcs of zeros in the ''northwest'' and ''southwest'' quadrants, and the points a_e, a_e^* lie near the ends of these arcs. In Fig. 1(a) there is more scatter among the zeros, but, nevertheless, the points a_e, a_e^* lie at the ends of subsets of zeros that can be associated with arcs. We have also performed analogous calculations of zeros on smaller lattices with similar results. For comparison, in Fig. 1(c) we show an exploratory calculation with type-3 DBC's. Taking into account that the lattice for

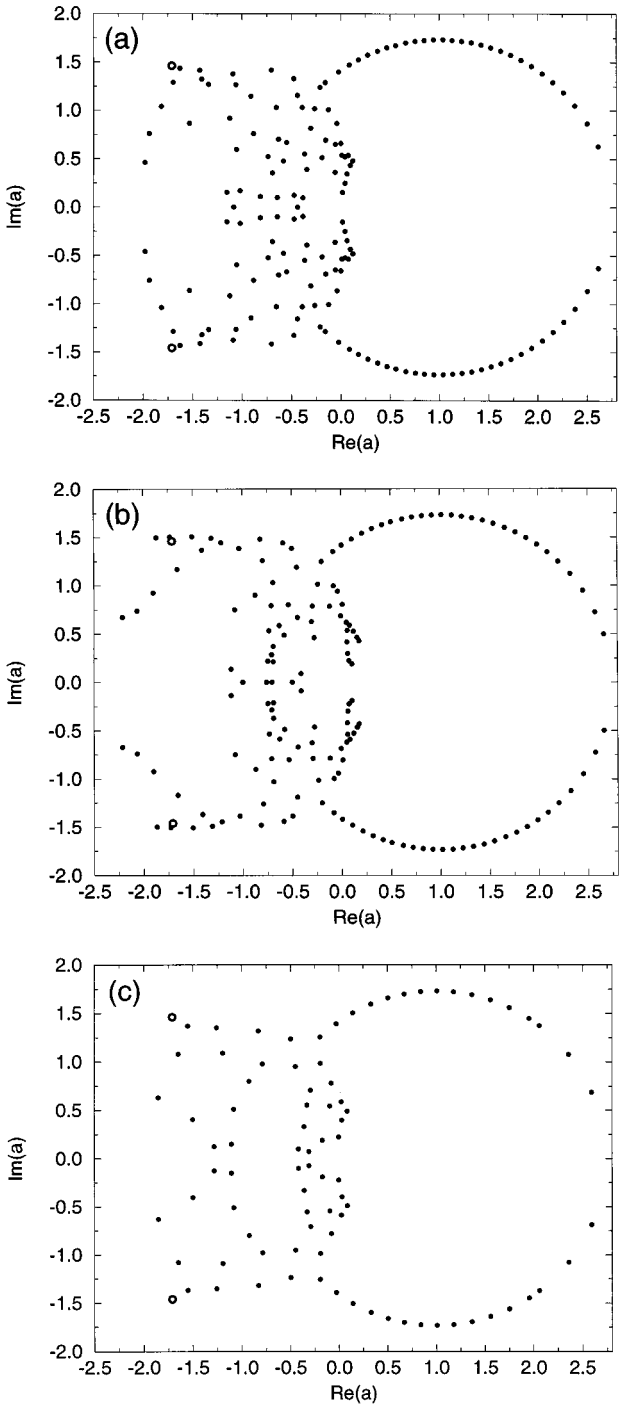

FIG. 1. Plot of zeros of Z, in the a plane, for the square-lattice $q=3$ Potts model on an 8×10 lattice with duality-preserving boundary conditions (DBC's) of (a) type 1, (b) type 2, and (c) on a 7×6 lattice with type-3 DBC's. The singularities a_e, a_e^* are marked with $\circ$.

Fig. 1(c) is somewhat smaller than that for Figs. 1(a) and 1(b), one sees that the distribution of zeros is similar to that in Fig. 1(a) with type-1 DBC's, especially in the region near a_e, a_e^* and their dual images. From all of these calculations, we thus conclude that the observed patterns of zeros are consistent with the hypothesis that in the thermodynamic limit, the points a_e, a_e^* are the ends of arcs contained in the complex-temperature boundary $\mathcal{B}$ which protrude into the FM phase. By duality, this is equivalent to the statement that the singularities at $\mathcal{D}(a_e), \mathcal{D}(a_e^*)$ are the endpoints of arcs contained in $\mathcal{B}$ which protrude into the PM phase.

F. Singularities at $a=0$ and $a=-2$

The exact solution (11) by Baxter shows that the point $a=0$, i.e., $T=0$ for $J<0$, is the antiferromagnetic critical point. By the duality property (14), it follows that the free energy is also singular, with the same singularity, at the dual to this point, namely, $a=-2\equiv a_s$ given in Eq. (12). From renormalization-group methods, a mapping to a critical six-vertex model, and studies of correlation functions, it has been concluded that the AFM critical point is an essential singularity, with an essential zero in the free energy and an exponential divergence in the correlation length as $K\to-\infty$, i.e., $a\searrow 0$ [41]. Thus, if one assigns algebraic exponents α and ν for this AFM critical point, then $\alpha=-\infty$, $\nu=\infty$. By duality, the same singularity in the free energy occurs at the dual point $a=-2$.

We have addressed two questions concerning these singularities at $a=0$ and -2: (i) how do they connect with the complex-temperature phase boundary $\mathcal{B}$ and (ii) how well do the low-temperature series detect the CT singular point at $a=-2$? For question (i), we first recall that the density g of CT zeros along the curves comprising $\mathcal{B}$ in the vicinity of a generic singular point a_s behaves as [13]

$$g\sim|a-a_s|^{1-\alpha_s}, \tag{25}$$

where a_s denotes a singular point and α_s (α_s') denotes the corresponding specific-heat exponent for the approach to a_s from within the CTE PM (FM) phase. Since $\alpha=-\infty$ at $a=0$ and hence, by duality, $\alpha_s'=-\infty$ at $a_s=-2$, there is a strong reduction in the density of CT zeros as one approaches these respective points $a=0$ and $a=-2$ along $\mathcal{B}$. This is consistent with what is observed with CT zeros calculated on finite lattices; one sees clear arcs of zeros and, e.g., for type-1 duality-preserving boundary conditions, these track toward the respective points $a=0$ and $a=-2$, ending some distance away from these points. (For type-2 DBC's, one also observes a slight curling tendency among the last few points on the curves.) From this tracking of the zeros toward $a=0$ (and hence, by duality, toward $a=-2$), we infer that the AFM critical point $a=0$ lies on a portion of $\mathcal{B}$ that connects with the continuation of the curves lying on (either part or all of) the unit circle $|a-1|=\sqrt{3}$ in such a way as to bound completely the complex-temperature extension of the PM phase. This is reminiscent of another model that has no AFM long-range order at any finite temperature, but an AFM critical point at $T=0$ [42], namely, the (isotropic, spin-1/2) Ising model on a triangular lattice. In that case, in terms of the variable $u=e^{-4K}$, the complex-temperature phase boundary $\mathcal{B}$ consists of the union of the circle $|u+1/3|=2/3$ and the semi-infinite line segment running along the negative real u axis from $-1/3$ to $-\infty$, or, equivalently, in the variable u^{-1} analogous to a, it consists of the union of the circle $|u^{-1}-1|=2$ and the line segment $-3\leq u^{-1}\leq 0$. The AFM critical point at $u^{-1}=0$ forms the right-hand end of this line segment and is connected to the rest of $\mathcal{B}$ by it. It is interesting to contrast this with the

TABLE V. Values of z_s and γ_s' from diagonal d log Padé approximants to low-temperature series for $\overline{\chi}$ for $q=3$.

$[N/D]$	z_s	γ_s'
[14/14]	−0.478716	1.66
[15/15]	−0.490833	2.31
[16/16]	−0.487890	2.12
[17/17]	−0.487889	2.12
[18/18]	−0.487906	2.12
[19/19]	−0.487844	2.11
[20/20]	−0.487995	2.12
[21/21]	−0.485409	1.99

situation in a model that is disordered and noncritical at $K=-\infty$, i.e., at $u^{-1}=0$. An example is provided by the (isotropic, spin-1/2) Ising model on the $3\cdot 6\cdot 3\cdot 6$ (Kagomé) lattice [43,44]. Since the point $u^{-1}=0$ is noncritical, it must be true that this point is not connected to $\mathcal{B}$, and indeed one finds [18,21] that it lies in the interior of the symmetric PM phase. The same behavior is found for the $3\cdot 12^2$ lattice [21].

Returning to the $q=3$ Potts model, the property that the AFM critical point at $a=0$ is connected to the rest of $\mathcal{B}$ as described above implies, by duality, that the singular point at $a=-2$ lies on the dual image of the above-mentioned curve, which therefore encloses a complex-temperature phase and separates it completely from the (CTE of the) FM phase. Given the scatter of the zeros, it is not possible to make a very reliable inference for where these curves intersect the continuation of the circle $|a-1|=\sqrt{3}$ in the northwest and southwest quadrants of the complex a plane. We do remark that the zeros are consistent with the possibility that these intersection points are $a=e^{\pm 2\pi i/3}$.

As regards the analysis of the low-temperature series, we find that these series are able to locate the singular point at $a_s=-2$, i.e., $z_s=-1/2$, but not very accurately. Representative results for diagonal d log Padé approximants are given in Table V, again based on the series calculated to $O(z^{47})$ in Ref. [35]. We do not show the results of the d log Padé approximants $[N/D]$ with $N=D<13$ because these did not locate the $z=-1/2$ singularity with acceptable accuracy (e.g., the [12/12] and [13/13] approximants gave $-0.607\,830$ and $-0.572\,062$, respectively). As is evident from Table V, the series yield values of the susceptibility exponent $\gamma_s'\sim 2$. Our previous work [19] has shown that there are subtleties in applying exponent relations such as $\nu' d=2-\alpha'$ and $\gamma'=\nu'(2-\eta)$ at complex-temperature singularities. However, it is of interest to note that, since $\alpha_s'=-\infty$, if the hyperscaling relation $\nu_s' d=2-\alpha_s'$ is valid, then $\nu_s'=\infty$ and hence, assuming that the relation $\gamma_s'=\nu_s'(2-\eta_s)$ holds at z_s, it would follow that $\gamma_s'=\infty$, i.e., χ would have an exponential divergence at this point. Of course, the series analysis cannot yield $\gamma_s'=\infty$, but it does produce a rather large value. For reference, one may recall that in the case of the 2D $O(2)$ model, while the Kosterlitz-Thouless theory implies that χ diverges exponentially as $T\searrow T_c$, so that $\gamma=\infty$, the earlier series analyses gave a value of roughly $\gamma=3$ [45].

G. Singularity at $a=1-3^{1/2}$

The Baxter solution (10) shows that the free energy is also singular at the self-dual complex-temperature point a_l given in Eq. (9) for $q=3$, viz., $a=1-\sqrt{3}$. There is considerable scatter of zeros in the vicinity of this point [less for our Fig. 1(c) or Fig. 11.1 of Ref. [30] than in Fig. 1(b)]; however, the zeros are consistent with the inference that this singular point lies on a segment of the circle $|a-1|=\sqrt{3}$. As one approaches the regions near the intersection points discussed above, the scatter of zeros becomes too great to draw a firm conclusion about this part of $\mathcal{B}$. Nevertheless, we are able to infer that the point a_l is completely separated from the FM phase by portions of the CT phase boundary $\mathcal{B}$. To see this, assume the contrary, i.e., that one can analytically continue from $z=0$ to $z_l=1/a_l$. First, this would contradict the property that the singular point at $a=-2$ lies on a portion of $\mathcal{B}$ connecting it to the rest of $\mathcal{B}$ (the dual image of the curve connecting the physical AFM critical point to the rest of $\mathcal{B}$). Second, if a_l were not completely separated from the FM phase, then one should be able to detect this singular point with the very long low-temperature series available. However, we found no evidence for a singularity at this point from our analysis of these series. The obvious conclusion is that a_l lies in a region beyond the applicability of these series, i.e., beyond the border of the (CTE) FM phase.

H. A Comment on dim($\mathcal{B}$) for Re(a)<0

We comment here on another feature of the pattern of zeros. For the 2D spin-1/2 Ising model with isotropic spin-spin couplings, one knows from exact solutions that on most lattices, the zeros merge to form a one-dimensional algebraic variety, i.e., the CT phase boundary $\mathcal{B}$. Even for isotropic couplings, there is a heteropolygonal lattice, i.e., the $4\cdot 8^2$ lattice, for which this is not the case; the locus of points where the free energy is nonanalytic forms a two-dimensional algebraic variety [21]. Moreover, for nonisotropic spin couplings, this is also true, even on the square lattice [46]. In both cases it is easy to see why this is true (see Sec. 6 of Ref. [21]). The zeros of the 2D Ising model for higher spin values also appear to approach curves as the lattice size gets large [23]. For the 2D q-state Potts model, the zeros in the Re(a)>0 half plane lie on a one-dimensional curve, i.e., part of a circle [28–32]. In the Re(a)<0 region, we are not aware of any proof of this. However, we can observe that in the known cases with exact solutions, in the thermodynamic limit, the zeros form either (i) curves or (ii) areas, but not both curves and areas. Thus, given that the zeros for Re(a)>0 do form a curve, one would have a qualitatively new situation not previously encountered if some of the zeros in the Re(a)<0 did form areas.

IV. $q=4$ POTTS MODEL

We have carried out exploratory analyses for higher-q Potts models on the square lattice and have found evidence for singularities analogous to z_e, z_e^* in each of the cases studied. We begin with the $q=4$ model. Like the $q=2,3$ cases, this model has a continuous, second-order PM-FM transition. However, from the exact solution by Baxter on the manifold (11), it follows that the $q=4$ model does not have any AFM

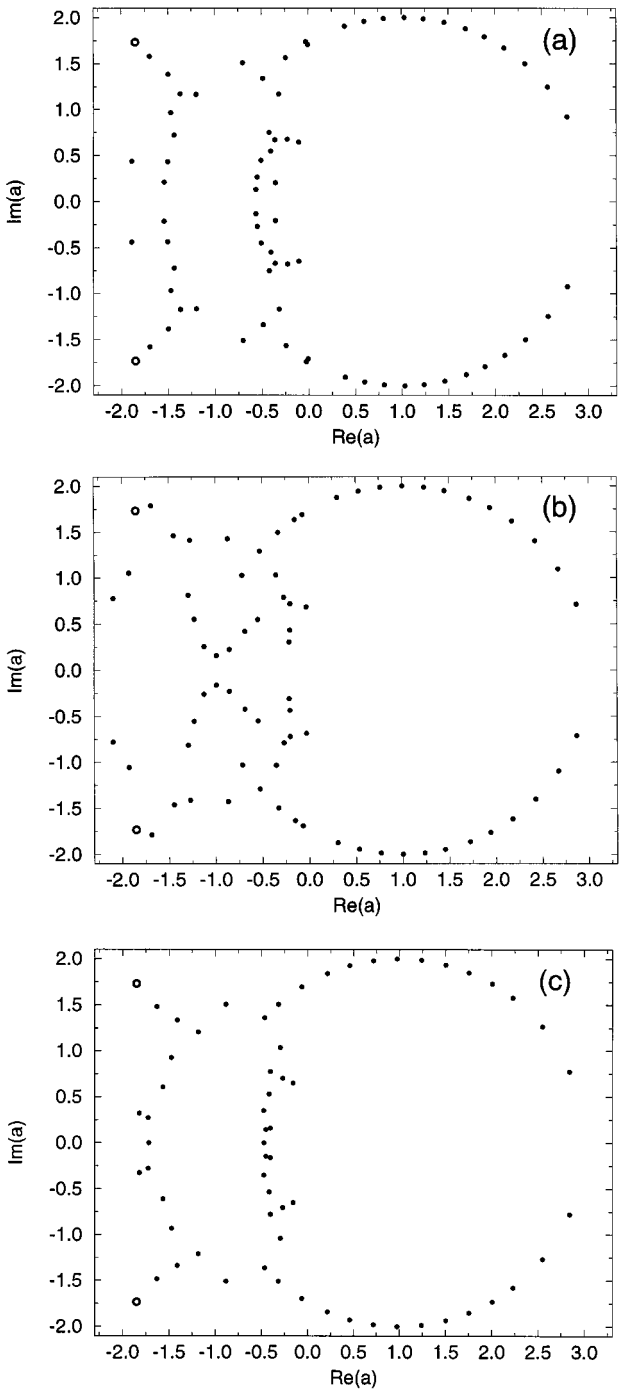

FIG. 2. Plot of zeros of Z, in the a plane, for the square-lattice $q=4$ Potts model on a 6×6 lattice with DBC's of (a) type 1, (b) type 2, and (c) on a 6×5 lattice with DBC's of type 3. The notation is the same as in Fig. 1.

critical point. Note that the complex-temperature point $a=-1$ lies on the manifold (11).

We have analyzed the low-temperature series for the magnetization, susceptibility, and specific heat as before. These yield a consistent indication of singularities at the points listed in Table IV. (The values of z_e from the χ series exhibit somewhat greater scatter than those from the m and C series.) It is interesting that, to within the uncertainty, our numerical value for $\mathrm{Im}(a_e^*)$ can be fit by the exact expression

TABLE VI. Values of z_e and β_e from d log Padé approximants to low-temperature series for m, for $q=5$.

$[N/D]$	z_e	β_e
[10/10]	$-0.248723+0.250655i$	-0.1023
[11/10]	$-0.248197+0.250780i$	-0.1004
[10/11]	$-0.248617+0.250694i$	-0.1019
[11/11]	$-0.249536+0.249950i$	-0.1034
[12/11]	$-0.251131+0.250021i$	-0.1105
[11/12]	$-0.251182+0.250694i$	-0.1142
[12/12]	$-0.251032+0.250976i$	-0.1146
[13/12]	$-0.250982+0.250979i$	-0.1143
[12/13]	$-0.250978+0.250974i$	-0.1142
[13/13]	$-0.251028+0.250979i$	-0.1146
[14/13]	$-0.251528+0.251159i$	-0.1190
[13/14]	$-0.251281+0.250904i$	-0.1157
[14/14]	$-0.251527+0.251148i$	-0.1189
[15/14]	$-0.251527+0.251158i$	-0.1190
[14/15]	$-0.251475+0.251197i$	-0.1188
[15/15]	$-0.251524+0.251171i$	-0.1190
[16/15]	$-0.251529+0.251161i$	-0.1190
[15/16]	$-0.251667+0.251138i$	-0.1199
[16/16]	$-0.251668+0.251140i$	-0.1199
[17/16]	$-0.251631+0.251079i$	-0.1191
[16/17]	$-0.251667+0.251138i$	-0.1199
[17/17]	$-0.251710+0.251167i$	-0.1205
[18/17]	$-0.251396+0.251142i$	-0.1181
[17/18]	$-0.251644+0.251144i$	-0.1198
[18/18]	$-0.252009+0.251663i$	-0.1282
[19/18]	$-0.251915+0.251720i$	-0.1267
[18/19]	$-0.251910+0.251717i$	-0.1266
[19/19]	$-0.251929+0.251724i$	-0.1270

$\mathrm{Im}(a_e^*)=\sqrt{3}$ for $q=4$. This and a similarly intriguing result that we find for $q=5$ suggest that there may be simple algebraic formulas for the singularities a_e, a_e^*. In view of the logarithmic confluent singularities that are known to occur at the physical PM-FM transition in this model [47], it would be useful in future work to carry out a more sophisticated analysis of the series including such confluent singularities also at the complex-temperature singularities; however, in the present exploratory work we have not done this. From our study of the low-temperature series for m, we find the exponent $\beta_e=-0.12(1)$, so that, as before, the magnetization diverges at z_e, z_e^*. This rigorously implies [24] that χ also diverges at these points.

In order to see how these singularities connect to the complex-temperature phase boundary $\mathcal{B}$ for the model, we have carried out a calculation of CT zeros of the partition function on various lattices with duality-preserving boundary conditions. In Figs. 2(a) and 2(b) we show calculations of these zeros, in the complex a plane, for a 6×6 lattice with type-1 and type-2 DBC's, respectively. Previously published calculations of zeros for this model include plots for strips ($L_x\times32$ for $L_x=4$, 6, and 8; and 10×16) [29] and a plot for a 4×4 lattice with type-2 DBC's. We use symmetric lattices since in taking the thermodynamic limit on an $L_x\times L_y$ lattice, if L_x/L_y deviates strongly from unity, the results can involve one-dimensional artifacts. For type-1 DBC's [Fig. 2(a)] one

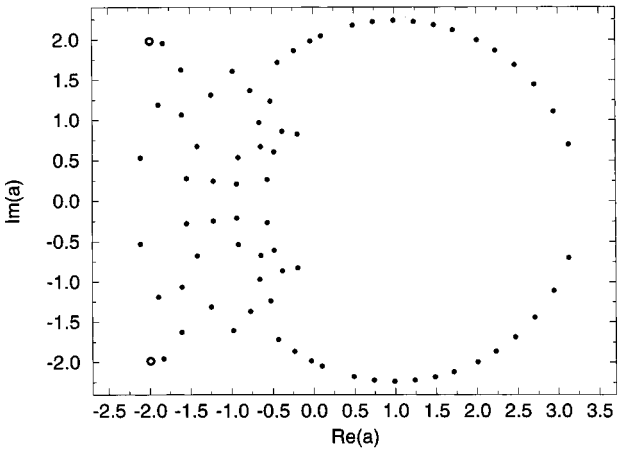

FIG. 3. Plot of zeros of Z, in the a plane, for the square-lattice $q=5$ Potts model on a 6×6 lattice with DBC's of type 2. The notation is the same as in Fig. 1.

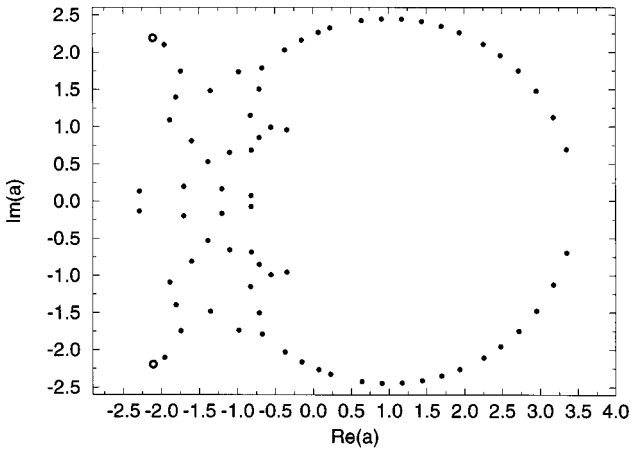

FIG. 4. Plot of zeros of Z, in the a plane, for the square-lattice $q=6$ Potts model on a 6×6 lattice with DBC's of type 2. The notation is the same as in Fig. 1.

sees a clear indication of a complex-conjugate pair of arcs of zeros in the northwest and southwest quadrants, with the singularities at a_e, a_e^* forming the endpoints of these arcs. These arcs are not as clear with type-2 DBC's [Fig. 2(b)], but again, the points a_e, a_e^* lie at the ends of subsets of zeros that can be associated with arcs. A calculation with type-3 DBC's is included as Fig. 2(c). The resultant pattern is very similar to that in Fig. 2(a) with type-1 DBC's, to an even greater extent than in the $q=3$ model. The patterns of zeros in Figs. 2(a)–2(c) are all in good agreement with the above-mentioned property that the model is not critical even at $a=0$, i.e., that it has no AFM critical point even at $T=0$. For the plot in Fig. 2(b) with type-2 DBC's, the zeros are consistent with the expectation from the Baxter solution (11) that the complex-temperature phase boundary $\mathcal{B}$ passes through the point $a=-1$ (equivalently for this $q=4$ case, $x=-1$). In contrast, for the plots in Figs. 2(a) and 2(c), with type-1 and type-3 DBC's, respectively, there are no zeros near, or easily extrapolated toward, $a=-1$. A clarification of the situation in the vicinity of this point merits further study on larger lattices.

V. HIGHER-q POTTS MODEL

We proceed to square-lattice Potts models with $q\geq 5$, for which the physical PM-FM phase transition is first order. Of course, a series analysis does not, in general, yield an accurate determination of the location of the phase transition point for a first-order transition. However, there is no obvious reason why this should be a drawback for our study of the complex-temperature arc endpoint singularities z_e, z_e^* since these yield a strong signal in the form of a divergent magnetization. In Table VI we list the results for z_e and corresponding exponent β_e from diagonal d log Padé approximants to the low-temperature series for m. We obtain similar results for z_e from the susceptibility and specific-heat series. From these diagonal (and near-diagonal) d log Padé approximants, we obtain the value for z_e listed in Table IV. This is an intriguing result since, to within the uncertainty, our determination is consistent with the exact analytic formula

$$a_e, a_e^* = 2(-1 \mp i) \quad \text{for} \quad q=5. \tag{26}$$

Of course, in the absence of an exact solution of the model, we cannot exclude the possibility that this agreement is fortuitous, but it motivates one to think further about simple analytic expressions for the location of the arc endpoints that we have discovered. From our series analysis, we find that the magnetization diverges at these points with exponent $\beta_e=-0.11(1)$. As noted above, this implies [24] that $\overline{\chi}$ must also diverge at these points, and our analysis of the low-temperature series for $\overline{\chi}$ yields the exponent $\gamma_e'=1.2(1)$.

We find the same generic features for all of the q values that we have analyzed, viz., complex-conjugate singularities at points z_e, z_e^*. These thus appear to be a general feature of the q-state Potts model on the square lattice for $q\geq 3$. Besides the case $q=5$, we have made exploratory studies of the low-temperature expansions for the cases $q=6$, 7, and 8. We find $z_e, z_e^* = -0.23 \pm 0.24i$, $-0.21 \pm 23i$, and $z_e = -0.20 \pm 22i$ for $q=6$, 7, and 8, respectively. Thus the magnitude $|z_e|$ ($|a_e|$) decreases (increases) as q increases. Note that if, in the x plane, the complex-conjugate arcs retract toward their respective points of origin and finally disappear in the $q\to\infty$ limit, as is required in order for the complex-temperature phase boundary $\mathcal{B}$ to reduce to the unit circle $|x|=1$ in this limit, it is necessary that for large q, $|\mathrm{Re}(a_e)|$ and $|\mathrm{Im}(a_e)|$ grow like $\sqrt{q}$. We find that β_e increases from ~ -0.11 for $q=6$ to ~ -0.10 for $q=8$.

In Figs. 3 and 4 we show our calculation of CT zeros of Z for $q=5$ and $q=6$ on a 6×6 lattice with type-2 DBC's. (We have checked that other DBC's give results which also support our conclusions.) Although there is considerable scatter of zeros in the $\mathrm{Re}(a)<0$ region, the pattern is again consistent with the conclusion that the singularities at a_e, a_e^* lie at the end of arcs of zeros, so that in the thermodynamic limit these points are endpoints of arcs of singularities that connect with the rest of the complex-temperature phase boundary $\mathcal{B}$.

VI. CONCLUSION

In summary, we have used analyses of low-temperature series expansions to study complex-temperature singularities in the square-lattice q-state Potts model. We have found singularities at complex-conjugate pairs of points and, by means of comparison with patterns of partition function zeros, have obtained support for the inference that in the thermodynamic limit these are endpoints of arcs lying on the complex-temperature phase boundary $\mathcal{B}$. At these points, the magnetization diverges, in agreement with an earlier conjecture that we had formulated. This guarantees that the susceptibility also diverges at these points, and our series analyses are in accord with this. Our work includes several intriguing findings, including the likely exponent value $\beta_e = -1/8$ for $q=3$ and an inference of an exact formula (26) for the endpoint singularities for $q=5$. From the duality of the model, it follows that these arcs protruding into the complex-temperature extension of the FM phase are accompanied by their dual images, i.e., arcs protruding into the CT extension of the PM phase. Our results further elucidate the complex-temperature phase diagrams of square-lattice Potts models.

ACKNOWLEDGMENTS

We thank Professor F. Y. Wu for the helpful private communication [34] and Professor A. J. Guttmann for a helpful comment. This research was supported in part by the NSF Grant No. PHY-93-09888.

[1] R. B. Potts, Proc. Cambridge Philos. Soc. **48**, 106 (1952).
[2] C. Domb, J. Phys. A **7**, 1335 (1974).
[3] S. Alexander, Phys. Lett. **54A**, 353 (1975); A. N. Berker, S. Oslund, and F. Putnam, Phys. Rev. B **17**, 3650 (1978); E. Domany, M. Schick, J. S. Walker, and R. B. Griffiths, *ibid.* **18**, 2209 (1978).
[4] R. J. Baxter, J. Phys. C **6**, L445 (1973); R. J. Baxter, H. N. V. Temperley, and S. Ashley, Proc. R. Soc. London Ser. A **358**, 535 (1978); R. J. Baxter, J. Stat. Phys. **28**, 1 (1982).
[5] R. J. Baxter, Proc. R. Soc. London Ser. A **383**, 43 (1982).
[6] M. P. M. den Nijs, J. Phys. A **12**, 1857 (1979); Phys. Rev. B **27**, 1674 (1982); J. L. Black and V. J. Emery, *ibid.* **23**, 429 (1981); B. Nienhuis, J. Appl. Phys. **15**, 199 (1982).
[7] A. A. Belavin, A. M. Polyakov, and A. B. Zamolodchikov, Nucl. Phys. B **241**, 333 (1984); D. Friedan, Z. Qiu, and S. Shenker, Phys. Rev. Lett. **52**, 1575 (1984); V. S. Dotsenko, Nucl. Phys. B **235**, 54 (1984). For nonunitary conformal field theories, see, e.g., G. von Gehlen, Int. J. Mod. Phys. B **8**, 3507 (1994), and references therein.
[8] F. Y. Wu, Rev. Mod. Phys. **54**, 235 (1982).
[9] C. N. Yang and T. D. Lee, Phys. Rev. **87**, 404 (1952); T. D. Lee and C. N. Yang, *ibid.* **87**, 410 (1952).
[10] M. E. Fisher, *Lectures in Theoretical Physics* (University of Colorado Press, Boulder, CO, 1965), Vol. 7C, p. 1.
[11] S. Katsura, Prog. Theor. Phys. **38**, 1415 (1967); Y. Abe and S. Katsura, *ibid.* **43**, 1402 (1970).
[12] S. Ono, Y. Karaki, M. Suzuki, and C. Kawabata, J. Phys. Soc. Jpn. **25**, 54 (1968).
[13] R. Abe, Prog. Theor. Phys. **38**, 322 (1967).
[14] C. J. Thompson, A. J. Guttmann, and B. W. Ninham, J. Phys. C **2**, 1889 (1969); A. J. Guttmann, *ibid.*, **C2**, 1900 (1969); C. Domb and A. J. Guttmann, J. Phys. C **3**, 1652 (1970).
[15] A. J. Guttmann, J. Phys. A **8**, 1236 (1975).
[16] R. B. Pearson, Phys. Rev. B **26**, 6285 (1982); C. Itzykson, R. B. Pearson, and J. B. Zuber, Nucl. Phys. B **220**, 415 (1983).
[17] G. Marchesini and R. Shrock, Nucl. Phys. B **318**, 541 (1989).
[18] R. Abe, T. Dotera, and T. Ogawa, Prog. Theor. Phys. **85**, 509 (1991).
[19] V. Matveev and R. Shrock, J. Phys. A **28**, 1557 (1995).
[20] V. Matveev and R. Shrock, J. Phys. A **28**, 4859 (1995).
[21] V. Matveev and R. Shrock, J. Phys. A **28**, 5235 (1995).
[22] V. Matveev and R. Shrock, Phys. Rev. E **53**, 254 (1996).
[23] V. Matveev and R. Shrock, J. Phys. A **28**, L533 (1995); Phys. Lett. A **204**, 353 (1995).
[24] V. Matveev and R. Shrock, J. Phys. A **29**, 803 (1996).
[25] I. G. Enting, A. J. Guttmann, and I. Jensen, J. Phys. A **27**, 6963 (1994).
[26] I. Jensen, A. J. Guttmann, and I. G. Enting, Report No. cond-mat/9604080.
[27] J. M. Maillard and R. Rammal, J. Phys. A **16**, 353 (1983).
[28] P. P. Martin and J. M. Maillard, J. Phys. A **19**, L547 (1986).
[29] P. P. Martin, J. Phys. A **19**, 3267 (1986); **20**, L601 (1986).
[30] P. P. Martin, *Potts Models and Related Problems in Statistical Mechanics* (World Scientific, Singapore, 1991).
[31] C. N. Chen, C. K. Hu, and F. Y. Wu, Phys. Rev. Lett. **76**, 169 (1996).
[32] F. Y. Wu, G. Rollet, H. Y. Huang, J. M. Maillard, C. K. Hu, and C. N. Chen, Phys. Rev. Lett. **76**, 173 (1996).
[33] The $q=\infty$ limit of the Potts model is solvable; see P. A. Pearce and R. B. Griffiths, J. Phys. A **13**, 2143 (1980). For some expansions in $1/\sqrt{q}$, see T. Bhattacharya, R. Lacaze, and A. Morel, Report No. hep-lat/9601012, and references therein.
[34] Our type-2 DBC's turn out to be the same as one of the DBC's alluded to in the reference to unpublished calculations of zeros with other DBC's (the other being type 3) in Ref. [31]. We thank Professor F. Y. Wu for kindly informing us of this and suggesting that we try his type-3 DBC's.
[35] K. M. Briggs, I. G. Enting, and A. J. Guttmann, J. Phys. A **27**, 1503 (1994).
[36] T. Kihara, Y. Midzuno, and T. Shizume, J. Phys. Soc. Jpn. **9**, 681 (1954); J. Straley and M. E. Fisher, J. Phys. A **6**, 1310 (1973); J. Adler, I. G. Enting, and V. Privman, *ibid.* **16**, 1967 (1982). See Ref. [35] for further references.
[37] G. Bhanot, M. Creutz, U. Glässner, I. Horvath, J. Lacki, K. Schilling, and J. Weckel, Phys. Rev. B **48**, 6183 (1993).
[38] The results obtained in Ref. [5] involved a mapping from the Potts model to a six-vertex model. A complication pertaining to a mismatch between the boundary conditions for the Potts and vertex model was noted there. See also H. Saleur, Commun. Math. Phys. **132**, 657 (1990).
[39] M. P. N. den Nijs, Physica A **95**, 449 (1979).
[40] A. J. Guttmann, in *Phase Transitions and Critical Phenomena*, edited by C. Domb and J. Lebowitz (Academic, New York, 1989), Vol. 13.

[41] M. P. Nightingale and M. Schick, J. Phys. A **15**, L39 (1982); M. P. M. den Nijs, M. P. Nightingale, and M. Schick, Phys. Rev. B **26**, 2490 (1982); J.-S. Wang, R. H. Swendsen, and R. Kotecký, *ibid.* **42**, 2465 (1990); S. J. Ferreira and A. D. Sokal, *ibid.* **51**, 6727 (1995).

[42] The criticality at $K=-\infty$ is evident, e.g., from the fact that $\langle\sigma_0\sigma_r\rangle$ decays like a power $r^{-1/2}$ (multiplied by an oscillatory trigonometric factor) rather than exponentially; see J. Stephenson, J. Math. Phys. **5**, 1009 (1964); **11**, 420 (1970).

[43] An Archimedean heteropolygonal lattice is defined by the symbol $p_1,\ldots,p_n$, meaning that as one makes a circuit around a site on the lattice, one traverses the polygons $p_1,p_2,\ldots,p_n$; see Ref. [21].

[44] K. Kano and S. Naya, Prog. Theor. Phys. **10**, 158 (1953); A. Sütö, Z. Phys. B **44**, 121 (1981).

[45] H. E. Stanley and T. Kaplan, Phys. Rev. Lett. **17**, 913 (1966); M. A. Moore, *ibid.* **23**, 861 (1969).

[46] W. van Saarloos and D. Kurtze, J. Phys. A **17**, 1301 (1984); J. Stephenson and R. Couzens, Physica A **129**, 201 (1984); D. Wood, J. Phys. A **18**, L481 (1985); J. Stephenson, Physica A **136**, 147 (1986); J. Stephenson and J. van Aalst, *ibid.* **136**, 160 (1986).

[47] M. Nauenberg and D. J. Scalapino, Phys. Rev. Lett. **44**, 837 (1980); J. Cardy, M. Nauenberg, and D. J. Scalapino, Phys. Rev. B **22**, 2560 (1981).